We are IntechOpen, the world's leading publisher of Open Access books
Built by scientists, for scientists

6,900
Open access books available

186,000
International authors and editors

200M
Downloads

Our authors are among the

154
Countries delivered to

TOP 1%
most cited scientists

12.2%
Contributors from top 500 universities

CLARIVATE ANALYTICS

BOOK
CITATION
INDEX

INDEXED

WEB OF SCIENCE™

Selection of our books indexed in the Book Citation Index
in Web of Science™ Core Collection (BKCI)

Interested in publishing with us?
Contact book.department@intechopen.com

Numbers displayed above are based on latest data collected.
For more information visit www.intechopen.com

Spontaneous Nonlinear Scattering Processes in Silica Optical Fibers

Edouard Brainis
Université libre de Bruxelles
Belgium

1. Introduction

When light travels in a optical fiber, a fraction of its total power is always scattered to other wavelengths (or polarization) due to material non linearity. Whether that scattering is weak or strong, desirable or not, depends on the situation. One distinguishes (i) scattering stimulated by the presence of a seed wave (at another wavelength or polarization), (ii) spontaneous scattering, and (iii) amplified spontaneous scattering. Stimulated Raman scattering (SRS), stimulated Brillouin scattering (SBS) and four-wave mixing (FWM) are examples of stimulated scatterings. Those have been thoroughly studied in the past thirty years and are well summarized in classic nonlinear fiber optics textbooks, e.g. (Agrawal, 2007). Several chapters of this book also deal with specific aspects and applications of stimulated scattering. The present chapter focuses on *spontaneous* scattering processes, cases (ii) and (iii).

The chapter also concentrates on nonlinear scattering in *silica* fibers because nowadays those are the most common and widely used types of fibers. Gas-filled hollow core fibers (Benabid et al., 2005) and ion doped fibers (Digonnet, 2001) are not considered here, and it is assumed that the fiber has not been subjected to poling (Bonfrate et al., 1999; Huy et al., 2007; Kazansky et al., 1997), so that the main non linearity is of third order. In this context the most important spontaneous nonlinear scattering processes are

1. the spontaneous Raman scattering (RS),

2. the spontaneous Brillouin scattering (BS), and

3. the spontaneous four-photon scattering (FPS).

These phenomena play an important role in many applications of optical fibers. This role can be positive as in remote optical sensing (Alahbabi et al., 2005a;b; Dakin et al., 1985; Farahani & Gogolla, 1999; Wait et al., 1997). It can also be detrimental as in fiber optics telecommunication, where spontaneous nonlinear scattering processes contribute to decrease the signal-to-noise ratio (SNR) or in supercontinuum generation, where it limits the coherence and stability of the supercontinuum (Corwin et al., 2003; Dudley et al., 2006). In the emerging field of quantum photonics, fiber optical photon-pair sources are intrinsically based on the physics of the FPS (Amans et al., 2005; Brainis, 2009; Brainis et al., 2005), while at the same time RS is the main factor that limits the SNR (Brainis et al., 2007; Dyer et al., 2008; Fan & Migdall, 2007; Lee et al., 2006; Li et al., 2004; Lin et al., 2006; 2007; Rarity et al., 2005; Takesue, 2006).

This chapter reviews the physics of spontaneous nonlinear scattering processes in optical fibers. In Sec. 2, the physical origin of RS, BS and FPS in explained. Because those are pure

quantum mechanical effects, they cannot be properly described in the framework of classical nonlinear optics. A quantum mechanical treatment is presented in Sec. 3. Finally, in Sec. 4, the coupling between different scattering processes in considered.

2. Physics of nonlinear scattering processes in optical fibers

2.1 Raman scattering

Light at frequency ω_p traveling in an optical fiber, can excite the fiber molecules from ground to excited vibrational states. In amorphous silica fiber, vibrational states have energy $\hbar|\Omega|$ with $|\Omega|/(2\pi)$ in the 0-40 THz range. These energies (about 0.05 eV) being much smaller than the photon energy $\hbar\omega_p$, no direct excitation of the vibrational states is possible. However, the states can be excited through a second order *Raman transition* involving a second photon at frequency ω_s and a virtual state as shown in Fig. 1. The spontaneous inelastic scattering that converts a ω_p photon into a $\omega_s = \omega_p - |\Omega|$ photon and a vibrational excitation at frequency $|\Omega|$ is call a spontaneous *Stokes* process. If a vibrational state at frequency $|\Omega|$ is initially populated, the complementary process in which a ω_p photon is converted into a $\omega_a = \omega_p + |\Omega|$ photon is also allowed and called a spontaneous *anti-Stokes* process, see Fig. 1.
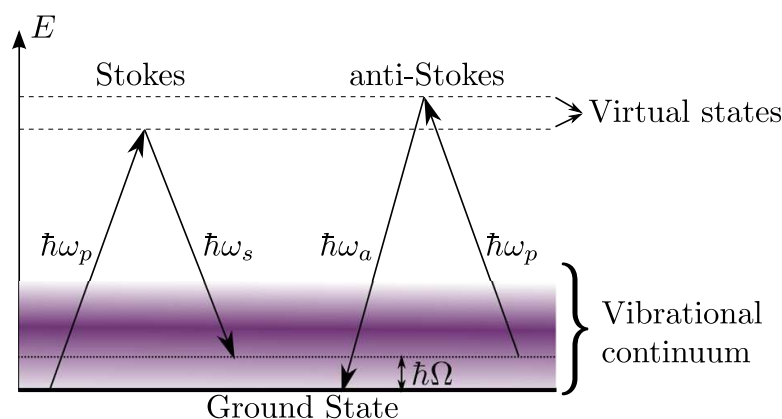

Fig. 1. Spontaneous Stokes and anti-Stokes processes in amorphous silica fibers

Molecular vibrations behave like waves (phonons). The momentum of these vibrational waves corresponds to the momentum mismatch of the pump and (anti-)Stoke waves and does not depend on $|\Omega|$. For this reason, Raman scattering has no preferential direction. It happens in the forward but also in the backward direction. The damping of a phonon wave depends on the wave number and is stronger for shorter wavelength. In fibers the damping is very strong because of the amorphous nature of silica. Therefore the molecular vibration can to a good approximation be considered as local. Yet the small difference in the forward and backward damping explains that the strengths of Raman scattering in forward and backward directions is slightly different (Bloembergen & Shen, 1964).

In addition to the Stokes and anti-Stokes processes that convert pump photons to other wavelengths, Raman scattering can also convert the Stokes and anti-Stokes photons at ω_s and ω_a back to the pump mode through *reverse* Stokes and anti-Stokes scattering. In Sec. 3.1, both direct and reverse scattering processes are taken into account to derive the basic equations governing the *net* energy transfer from the pump to Stokes and anti-Stokes waves. For a single monochromatic pump wave at ω_p the scattered spectral power density $\mathcal{S}(z,\omega)$ obeys

the following propagation equation

$$\frac{\mathrm{d}}{\mathrm{d}z}\mathcal{S}(z,\omega) = \left[\mathcal{S}(z,\omega)g(\omega_p,\Omega,\theta) + \frac{\hbar\omega}{2\pi}\left[m_{\text{th}}(|\Omega|) + \nu(\Omega)\right]|g(\omega_p,\Omega,\theta)|\right]P_p(z) \qquad (1)$$

where $\Omega = \omega_p - \omega$ (positive for a Stokes process and negative for an anti-Stokes ones), $\nu(\Omega)$ is the Heaviside step function, and

$$m_{\text{th}}(|\Omega|) = \left[\exp\left(\frac{\hbar|\Omega|}{k_B T}\right) - 1\right]^{-1} \qquad (2)$$

is the thermal equilibrium expectation value of the number of vibrational excitations at angular frequency $|\Omega|$. The function $g(\omega_p,\Omega,\theta)$ in Eq. (1) is the Raman *gain*. The Raman gain measures the scattering strength and is polarization dependent. For a linearly polarized pump field, the Raman gain is maximal for photon scattered with polarization parallel to the pump and minimal for photons scattered with polarization orthogonal to the pump (Stolen, 1979):

$$g(\omega_p,\Omega,\theta) = g_{\parallel}(\omega_p,\Omega)\cos^2(\theta) + g_{\perp}(\omega_p,\Omega)\sin^2(\theta), \qquad (3)$$

where θ is the angle between the linear polarization vectors of pump and scattered photons. The parallel and orthogonal gains are $g_{\parallel}(\omega_p,\Omega)$ and $g_{\perp}(\omega_p,\Omega)$ are material properties that can be measured experimentally. It can be shown (see Sec. 3.1) that the ratio of the Stokes to anti-Stokes gain corresponding to the same vibrational mode $|\Omega|$ is

$$\frac{g(\omega_p,\Omega,\theta)}{g(\omega_p,-\Omega,\theta)} = -\frac{n(\omega_p+|\Omega|)}{n(\omega_p-|\Omega|)}\left(\frac{\omega_p-|\Omega|}{\omega_p+|\Omega|}\right)^3. \qquad (4)$$

Stokes and anti-Stokes gain have opposite signs: Stokes gain is positive while anti-Stokes gain is negative.

2.1.1 Spontaneous scattering

With initial condition $\mathcal{S}(0,\omega) = 0$, $\forall\omega \neq \omega_p$, Eq. (1) describes both spontaneous Raman scattering and its subsequent amplification. In the initial propagation stage, the first term in the square bracket can be neglected. This regime corresponds to pure spontaneous Raman scattering. The solution of Eq. (1) is

$$\mathcal{S}(L,\omega) = \frac{\hbar\omega}{2\pi}\left[m_{\text{th}}(|\Omega|) + \nu(\Omega)\right]|g(\omega_p,\Omega,\theta)|P_p L, \qquad (5)$$

where L is the propagation length. The strength of the spontaneous Raman parallel and orthogonal scattering is often measured by the parallel and orthogonal *spontaneous Raman coefficients*

$$R_{\parallel,\perp}(\omega_p,\Omega,T) = \frac{\hbar\omega_p}{2\pi}\left[m_{\text{th}}(|\Omega|) + \nu(\Omega)\right]|g_{\parallel,\perp}(\omega_p,\Omega)|. \qquad (6)$$

Spontaneous Raman scattering has been observed and measured in bulk glass (Hellwarth et al., 1975; Stolen & Ippen, 1973) and in optical fibers (Stolen et al., 1984; Wardle, 1999). In optical fiber, the polarization properties are usually more difficult to measure because standard fibers do not preserve and even scramble polarization. For this reason, the *effective spontaneous Raman coefficient* is often taken to be $R = (R_{\parallel} + R_{\perp})/2$.

It is interesting to note that the ratio of Stoke to anti-Stokes spectral components only depend on temperature:

$$\frac{\mathcal{S}(L, \omega_p - |\Omega|)}{\mathcal{S}(L, \omega_p + |\Omega|)} = \frac{n(\omega_p + |\Omega|)}{n(\omega_p - |\Omega|)} \left(\frac{\omega_p - |\Omega|}{\omega_p + |\Omega|} \right)^4 \exp \left(\frac{\hbar |\Omega|}{k_B T} \right). \tag{7}$$

This is the reason why spontaneous Raman scattering is used for temperature sensing (Alahbabi et al., 2005a;b; Dakin et al., 1985; Farahani & Gogolla, 1999; Wait et al., 1997).

2.1.2 Amplified spontaneous scattering

According to Eq. (1), the spontaneous scattering regime ends as soon as $\mathcal{S}(z, \omega)$ becomes significant compared to $\frac{\hbar \omega}{2\pi} [m_{\text{th}}(|\Omega|) + \nu(\Omega)]$. At that point, the scattering becomes stimulated and the system enters the amplification regime. From Eq. (5), one sees that the amplification regime is reached when $g(\omega_p, \Omega, \theta) \, P_p \, L \approx 1$. For $\mathcal{S}(0, \omega) = 0$, the solution of Eq. (1) is

$$\mathcal{S}(L, \omega) = \frac{\hbar \omega}{2\pi} [m_{\text{th}}(|\Omega|) + \nu(\Omega)] \left| e^{g(\omega_p, \Omega, \theta) \, P_p \, L} - 1 \right|. \tag{8}$$

Stokes radiation ($\Omega > 0$, $g > 0$) is *grows exponentially* while anti-Stokes ($\Omega > 0$, $g < 0$) radiation saturates at $\mathcal{S}(L, \omega) = \frac{\hbar \omega}{2\pi} m_{\text{th}}(|\Omega|)$. When losses are taken into account, the gain must overcome a threshold value to enter the amplification regime. Since the Raman gain is frequency dependent, the amplification bandwidth depends on the input power. The effective amplification threshold is usually considered to be reached when Stokes and pump intensity have the same value at the output of the fiber (Agrawal, 2007; Smith, 1972).

By measuring the grows of the Stokes wave, one can deduced the Raman gain as a function of frequency (Mahgerefteh et al., 1996; Stolen et al., 1984). Amplified spontaneous Stokes wave plays an important role in Raman fiber amplifiers (Aoki, 1988; Mochizuki et al., 1986; Olsson & Hegarty, 1986).

Fig. 2 shows the typical (forward) Raman gain $g_\parallel(\omega_p, \Omega)$ and the spontaneous Raman coefficient $R_\parallel(\omega_p, \Omega, T)$ in a silica fiber at $\lambda_p = 1.5$ μm. The parallel Raman gain has a peak at $\Omega_R = 13.2$ THz and a width of about 5 THz. The peak value varies for fiber to fiber. A typical value is $g_R = 1.6$ W^{-1} km^{-1}. The orthogonal gain $g_\perp(\omega_p, \Omega)$ is about 30 times smaller (Agrawal, 2007; Dougherty et al., 1995; Stolen, 1979). The parallel gain can be fit using a 10-Lorentzian model, each Lorentzian having three independent parameters : strength, central frequency, and width (Drummond & Corney, 2001). Note that spontaneous anti-Stokes scattering can be eliminated by lowering the temperature, while the spontaneous Stokes coefficient $R_\parallel$ is at least $\hbar \omega_p / (2\pi) \times g_\parallel$.

2.2 Brillouin scattering

Brillouin scattering is very similar to Raman scattering in the sense it couples two light modes to material vibrations. However, in the contrast with Raman scattering which couples light to molecular vibrations, Brillouin scattering couples light to vibration modes of the fiber itself, that is *sound* waves. Therefore the vibrational frequencies involved in Brillouin scattering are much lower: $|\Omega|/(2\pi)$ is usually in the 10 GHz range. BS is also polarization dependent: as long as the fiber can be considered as mechanically isotropic, their is no orthogonal BS, that is $g_\perp = 0$ (Benedek & Fritsch, 1966; McElhenny et al., 2008; Stolen, 1979). The major difference between Raman and Brillouin scattering lies in the dispersion relation of acoustics vibrations:

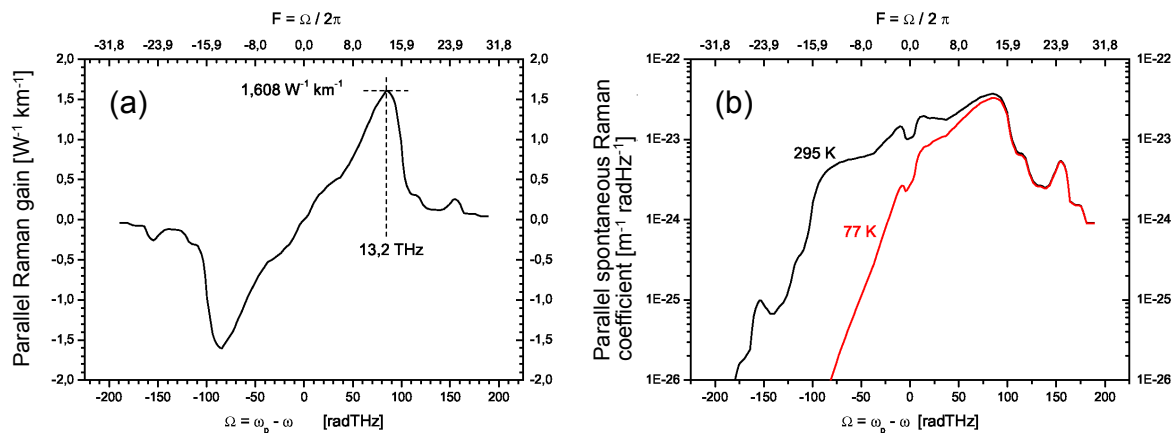$$|\Omega| = v_A \, |\mathbf{k}_A|, \tag{9}$$

Fig. 2. (a) Raman gain $g_\parallel$ in a silica fiber for $\lambda_p = 1.5$ μm and forward propagation. Peak value: $g_R = 1.6$ W^{-1} km^{-1}. Peak position: $\Omega_R = 13.2$ THz. (b) Spontaneous Raman coefficient $R_\parallel$ for $\lambda_p = 1.5$ μm and forward propagation at $T = 295$ K and 77 K.

where $v_A = 5.96$ km/s in silica fibers and $\mathbf{k}_A$ is the wave vector of the acoustic wave. Because of momentum conservation, $\mathbf{k}_A$ is equal to the wave vector mismatch between pump and (anti-)Stokes waves: $\mathbf{k}_A = \mathbf{k}_p - \mathbf{k}_{s,a}$. Since the energy difference between pump, Stokes and anti-Stokes waves is very small, $|\mathbf{k}_p| \approx |\mathbf{k}_{s,a}|$ and $|\mathbf{k}_A|^2 \approx 2|\mathbf{k}_p|^2 [1 - \cos(\phi)] = 4|\mathbf{k}_p|^2 \sin^2(\phi/2)$, where ϕ is the angle between $\mathbf{k}_p$ and $\mathbf{k}_{s,a}$. Eq. (9) yields

$$|\Omega| = 2\, v_A\, |\mathbf{k}_p|\, \sin^2(\phi/2) = 4\pi\, v_A\, \frac{n(\omega_p)}{\lambda_p}\, \sin^2(\phi/2). \tag{10}$$

The maximum value of $|\Omega|$ occurs for backward propagation ($\phi = \pi$), while for forward propagation of (anti-)Stokes waves ($\phi = 0$), $|\Omega| = 0$. Therefore, forward Brillouin scattering is not observed. In the backward direction the Brillouin gain as a peak is at $\Omega_R/(2\pi) = 11.1$ GHz when $\lambda_p = 1.55$ μm. The Brillouin gain has a Lorentzian spectrum

$$g_\parallel(\omega_p, \Omega) = \text{sign}(\Omega) \frac{g_B(\Gamma_B/2)^2}{(|\Omega| - \Omega_B)^2 + (\Gamma_B/2)^2} \tag{11}$$

and its spectral width $\Gamma_B/(2\pi)$ is in the 10-100 MHz range. $1/\Gamma_B$ is the decay time of the sound waves. The peak value g_B is usually of the order of 1000 W^{-1} km^{-1}, one thousand times higher than the Raman gain peak g_R.

The Brillouin gain spectrum discussed so far corresponds to a plane acoustic wave propagating along the fiber axis. Other smaller peaks may occur due to other acoustic modes, the presence of dopants and their spatial distribution (Lee et al., 2005; Yeniay et al., 2002). Guided acoustic wave can also produce narrow and very low frequency Brillouin shifts (50 kHz to 1 GHz) and can be even observed in the forward direction (Shelby et al., 1985a;b).

Despite the differences in the Raman and Brillouin gain functions, the underlying scattering mechanism is the same. Therefore, the principle explained in Sec. 3.1 in the context of RS also apply to BS. In particular spontaneous BS exhibits the same temperature dependence as spontaneous RS. Spontaneous Brillouin scattering can be used for temperature sensing (Alahbabi et al., 2005a;b; Pi et al., 2008; Wait et al., 1997).

2.3 Four-photon scattering

The four-photon scattering process differs from the previous scattering processes in that it involves four photons and no material vibration. Since a silica fiber is centro-symmetric, it is the lowest order nonlinear scattering phenomenon that involves only photons in the input and output channels. As shown in Fig. 3, a FPS process consists in the conversion
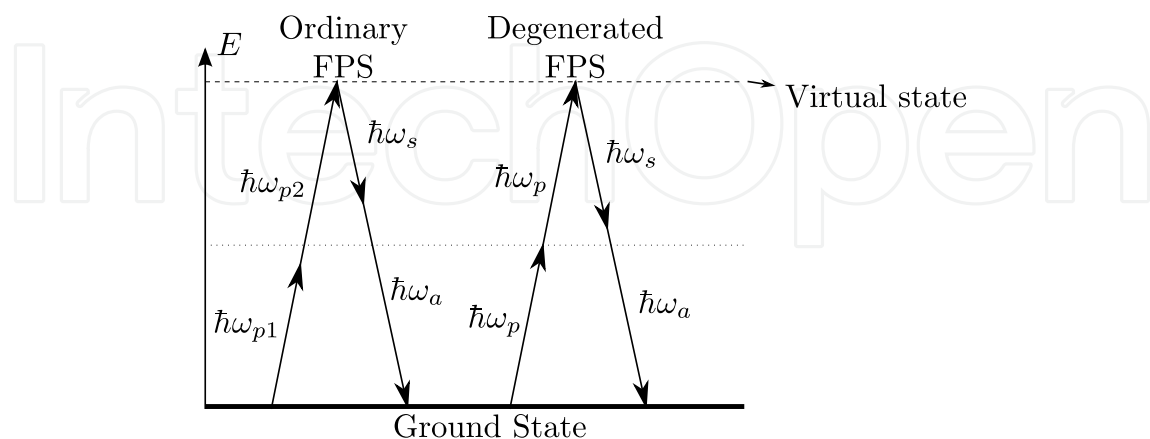

Fig. 3. Spontaneous four-photon scattering processes in silica fibers: ordinary and degenerated case.

of two pump photons at frequencies ω_{p1} and ω_{p2} into two other photons at frequencies ω_s and ω_a. The photon of lower energy is called "Stokes", the one of higher energy in called "anti-Stokes" as in the RS and BS processes. The conversion process satisfies the energy and moment conservation laws

$$\omega_{p1} + \omega_{p2} = \omega_s + \omega_a, \tag{12}$$

$$\mathbf{k}_{p1} + \mathbf{k}_{p2} = \mathbf{k}_s + \mathbf{k}_a. \tag{13}$$

When $\omega_{p1} = \omega_{p2}$ the FPS process is said to *degenerated* and is by far the most studied case, both experimentally and theoretically. FPS is a non resonant process. Therefore many different resonances can contribute to it. In silica, the main contribution comes from electronic resonances. Molecular vibrations contribute to a fraction $f_R = 18\%$ of the FPS strength.

The spectrum of a spontaneous FPS process is usually very broadband. It is not limited by resonance conditions (as RS) or losses (as BS), but merely by the phase matching conditions (13). If a single mode fiber, the wave number of a optical wave has a linear part $k_L(\omega) = n(\omega)\omega/c$ that depends on the effective index $n(\omega)$ of the mode, and a nonlinear part k_{NL} that depends on the power carried by the wave itself (self-phase modulation) and the power of the other waves propagation in the fiber (cross-phase modulation) (Agrawal, 2007). In a spontaneous FPS problem, Stokes and anti-Stokes waves are so faint that their contribution to self or cross-phase modulation is negligible. On the other hand, the pump wave modulates its own phase as well as the phases of the Stokes and anti-Stokes waves. If a wave carries a power P, self-phase modulation changes its own wave number by $k_{NL} = \gamma P$, where γ is the nonlinear coefficient of the fiber. At the same time, that wave modifies the wave number of any other co-polarized wave by $k_{NL} = 2\gamma P$ and any other orthogonally polarized wave by $k_{NL} = (2/3)\gamma P$, through the cross-phase modulation effect. For instance, for a degenerate co-polarized FPS, the wave number mismatch is $\Delta k = k_s + k_a - 2k_p = (k_{Ls} + 2\gamma P_p) + (k_{La} + 2\gamma P_p) - 2(k_{Lp} + \gamma P_p) = \Delta k_L + 2\gamma P_p$, where P_p is the pump power. Using quantum

perturbation theory (Brainis, 2009), it can be shown that the spectral density of power at Stokes and anti-Stokes wavelengths is

$$S(L, \omega_s) = S(L, \omega_a) = \frac{\hbar \omega_{s,a}}{2\pi} \left(\gamma P_p L \right)^2 \operatorname{sinc}^2 \left(\frac{\Delta k}{2} L \right) \tag{14}$$

in the case of degenerate co-polarized FPS. Equivalent formulas for non co-polarized degenerate FPS processes can be found in (Brainis, 2009). Whatever the FPS process (degenerated or not, co-polarized or not, ...), Stokes and anti-Stokes powers are always equal because those photons are created in pairs and the spectrum always depends on the wave number mismatch through the same sinc-function factor, see also Sec. 4.2.

It is important to note that the strength of a spontaneous FPS process scales as $(P_p L)^2$, while the strength of spontaneous RS and BS scales as $P_p L$. The spontaneous FPS spectrum is also independent on temperature. Increasing the propagation length L not only increases the amount of scattered photons, but also narrows the spectrum. In contrast, raising the pump power increases scattering, but as little impact of the spectrum. Therefore, adjusting both parameters, it is possible to set the spectral width of the Stokes and anti-Stokes waves as well as their intensities. Because Stokes and anti-Stokes photons are created in pair, FPS as been extensively studied in the context of photon-pair generation for quantum optics and quantum information applications (Amans et al., 2005; Brainis, 2009; Brainis et al., 2005; 2007; Dyer et al., 2008; Fan & Migdall, 2007; Lee et al., 2006; Li et al., 2004; Lin et al., 2006; 2007; Rarity et al., 2005; Takesue, 2006).

When the scattered intensity becomes high enough ($\gamma P_p \gtrsim 1$), spontaneous scattering gets amplified. In the case of the degenerate co-polarized FPS, the growth of Stokes and anti-Stokes waves in the amplification regime in described by (Brainis, 2009; Dyer et al., 2008)

$$S(L, \omega_s) = S(L, \omega_a) = \frac{\hbar \omega_{s,a}}{2\pi} \left(\gamma P_p L \right)^2 \left| \frac{\sinh \left(g(\omega_{s,a}) L \right)}{g(\omega_{s,a}) L} \right|^2, \tag{15}$$

where $g(\omega_{s,a}) = \sqrt{(\gamma P_p)^2 - (\Delta k/2)^2}$ is the *parametric gain* function that appears in the classical theory of four-wave mixing (Agrawal, 2007). Amplification only occurs at those frequencies for which $g(\omega_{s,a}) \in \mathbb{R}$. Because such a condition is never satisfied in the spontaneous regime ($g(\omega_{s,a}) \xrightarrow{P \to 0} i\sqrt{\Delta k_L \gamma P_p}$), it strongly modifies the FPS spectrum when amplification begins. It the amplified regime, the spectral width is determined by $g(\omega_{s,a})$ rather by the propagation length. The peak value of the parametric gain g_P is larger by 70% that the Raman peak gain g_R.

3. Quantum mechanical description of nonlinear scattering

Spontaneous scattering of light cannot be understood in the framework of classical nonlinear optics. A proper description requires the quantum theory. There are two possible approaches. The most elementary one consists in (i) applying quantum perturbation theory to calculate the scattering of light by a single molecule in the first place, then (ii) extending the result to continuous media. The drawback of this method is that it gives access the scattered power density, but not to the field amplitudes. The second approach consists in using a quantum field theory of propagation of light in the fiber that is based on an effective matter/light interaction Hamiltonian.

The "perturbation theory" approach is used in Sec. 3.1 to derive, from first principles, the main formula of Sec. 2.1 for RS. Having identified the limitations of that method, the "field theory method" will be presented in Sec. 3.2.

3.1 Perturbation theory of Raman scattering

The simplest way to model Stokes and anti-Stokes Raman scattering from a coherent pump wave at ω_p consists in applying second order perturbation theory (Crosignani et al., 1980; Wardle, 1999) to matter/light coupling described by the interaction Hamiltonian $H = -\mathbf{d} \cdot \mathbf{E}$, where

$$\mathbf{E}(\mathbf{r}, t) = i \frac{f(x,y)}{\sqrt{L}} \left[\sqrt{\frac{\hbar \omega_p}{2 \epsilon_0 n^2(\omega_p)}} \alpha_p \, e^{i(k(\omega_p)z - \omega_p t)} \mathbf{e}_p - c.c. + \sqrt{\frac{\hbar \omega}{2 \epsilon_0 n^2(\omega)}} a \, e^{i(k(\omega)z - \omega t)} \mathbf{e} - h.c. \right] \tag{16}$$

is the electric field operator associated to the light travelling in the fiber and $\mathbf{d}$ is the electronic dipole moment operator of a scattering fiber molecule at position $\mathbf{r}$. In Eq. (16), the field as been reduced to a pump mode in a coherent state with amplitude α (treated as a strong classical field) and a signal mode representing either the Stokes or anti-Stokes wave at frequency ω. The polarization of the pump and signal modes is defined by the unit vectors $\mathbf{e}_p$ and $\mathbf{e}$. In Eq. (16), the quantity L is the quantization length, a formal parameter that will disappear at the end of the calculation and $f(x,y)$ is normalized so that $\iint f^2(x,y) \mathrm{d}A = 1$, where the integration is over the entire fiber cross-section. This normalization is such that

$$\hbar \omega \frac{c}{n(\omega)L} \langle a^\dagger a \rangle = P(\omega) \quad \text{and} \quad \hbar \omega_p \frac{c}{n(\omega_p)L} |\alpha_p|^2 = P_p, \tag{17}$$

with P_p and $P(\omega)$ the powers in the pump mode and the signal mode, respectively.

The vibration of a molecule can be decomposed in normal modes. Assuming that only one normal mode is excited, the electronic dipole moment of the molecule can be written to first order as

$$\mathbf{d} = \mathbf{d}_0 + \mathbf{d}'Q, \tag{18}$$

where Q is the normal mode coordinate of the vibration, $\mathbf{d}_0$ the dipole moment around the molecular equilibrium point and $\mathbf{d}' = \frac{\partial \mathbf{d}}{\partial Q}$.

Consider the Stokes process first ($\omega < \omega_p$). Assuming that the molecule starts in the electronic ground state $|g\rangle$ and the vibrational number state $|m\rangle$ and that the Stokes mode is in the Fock state $|n\rangle$, the transition probability amplitude to the state $|g, m+1, n+1\rangle$ after an interaction time t can be calculated using *second* order perturbation theory (Wardle, 1999):

$$c(\Omega, m, n, t) = \frac{f^2(x,y)}{L} \, e^{i[k(\omega) - k(\omega_p)]z} \sqrt{\frac{\omega_p \omega}{8 \hbar \epsilon_0^2 n^2(\omega_p) n^2(\omega) M \Omega}} \sqrt{m+1} \sqrt{n+1} \, \alpha_p$$

$$[\mathbf{e}_p]^\dagger \cdot R \cdot \mathbf{e} \, \frac{e^{i(\Omega + \omega - \omega_p)t} - 1}{\Omega + \omega - \omega_p}, \tag{19}$$

where M and Ω are the effective mass and angular frequency of the molecular normal mode of vibration, while $R \approx 2 \sum_e \frac{1}{\omega_{eg}} \langle e | \mathbf{d} \otimes \mathbf{d}' + \mathbf{d}' \otimes \mathbf{d} | g \rangle$, where $\otimes$ denotes the tensor product of two vectors and the sum runs over all the electronic excited states of the scattering molecule having Bohr frequencies ω_{eg} with respect to the ground state.

Around each point $\mathbf{r}$, the material medium is made of many molecules and each molecule has several normal modes of vibration. Since all the molecules are at thermal equilibrium, their vibration have no locked phase relationship. The local field is thus simultaneously coupled to a large thermal reservoir of independent vibration modes and the contribution $c(\Omega, m, n, t)$ of each of them to the overall scattering probability can be added *incoherently*. Writing $\rho(\Omega)$ the number of vibration modes in the volume $\mathrm{d}V$ centered on $\mathbf{r}$ with a frequency in the interval $[\Omega, \Omega + \mathrm{d}\Omega]$ and and taking the thermal average of the number of excitations in a vibration mode Ω, the *Stokes scattering rate* from the point $\mathbf{r}$ (integrated over all the possible vibration modes frequencies Ω) is found to be

$$S(n; \mathbf{r}) = \frac{\mathrm{d}V}{L^2} f^4(x, y) \frac{\pi \omega_p \omega}{4\hbar \epsilon_0^2 n^2(\omega_p) n^2(\omega)} \frac{\rho(|\Omega|) \langle (\mathbf{e}_p^\dagger \cdot R \cdot \mathbf{e})^2 \rangle}{M|\Omega|} (m_{\mathrm{th}}(|\Omega|) + 1)(n + 1)|\alpha_p|^2, \quad (20)$$

where Ω is not an independent variable anymore but is now *defined* as $\Omega := \omega_p - \omega$, and $m_{\mathrm{th}}(|\Omega|)$ – given by Eq. (2) – is the Bose-Einstein expectation value of the number of vibrational excitations. The average $\langle (\mathbf{e}_p^\dagger \cdot R \cdot \mathbf{e})^2 \rangle$ is taken over arbitrary molecular orientation in amorphous silica. Therefore the quantity $\langle (\mathbf{e}_p^\dagger \cdot R \cdot \mathbf{e})^2 \rangle$ only depends on the angle θ between $\mathbf{e}_p$ and $\mathbf{e}$. As a result, one can write

$$\frac{\rho(|\Omega|) \langle (\mathbf{e}_p^\dagger \cdot R \cdot \mathbf{e})^2 \rangle}{M|\Omega|} = K_\parallel(|\Omega|) \cos^2(\theta) + K_\perp(|\Omega|) \sin^2(\theta) = K(|\Omega|, \theta), \quad (21)$$

where $K_\parallel(|\Omega|)$ and $K_\perp(|\Omega|)$ are material characteristics that can be determined experimentally[1]. The total scattering rate from ω_p to ω due to the Stokes process in a fiber segment $\mathrm{d}z$ is obtained by integration $S(n, \mathbf{r})$ over the fiber cross-section. As a consequence,

$$S_{p \to s}(n) = \mathrm{d}z \frac{\pi \omega_p \omega}{4\hbar \epsilon_0^2 n^2(\omega_p) n^2(\omega) A_{\mathrm{eff}} L^2} K(|\Omega|, \theta) (m_{\mathrm{th}}(|\Omega|) + 1) (n + 1) |\alpha_p|^2, \quad (22)$$

where $A_{\mathrm{eff}} = 1/ \left(\iint f^4(x, y) \mathrm{d}A \right)$ is the effective area of the fiber (Agrawal, 2007).
The scattering rate for the anti-Stokes process ($\omega > \omega_p$) can be computed according to the same lines: the rate is the same as in Eq. (22) with the exception that $(m_{\mathrm{th}}(|\Omega|) + 1)$ is replaced by $m_{\mathrm{th}}(|\Omega|)$ since an vibrational excitation is destroyed in that process:

$$A_{p \to a}(n) = \mathrm{d}z \frac{\pi \omega_p \omega}{4\hbar \epsilon_0^2 n^2(\omega_p) n^2(\omega) A_{\mathrm{eff}} L^2} K(|\Omega|, \theta) \, m_{\mathrm{th}}(|\Omega|) (n + 1) |\alpha_p|^2. \quad (23)$$

During propagation, light is not only scattered from the pump to the Stokes and anti-Stokes modes at $\omega_p - |\Omega|$ and $\omega_p + |\Omega|$ but also *from* these mode to the pump wave. The rates associated to these *reverse* Raman processes are

$$A_{s \to p}(n) = \mathrm{d}z \frac{\pi \omega_p \omega}{4\hbar \epsilon_0^2 n^2(\omega_p) n^2(\omega) A_{\mathrm{eff}} L^2} K(|\Omega|, \theta) \, m_{\mathrm{th}}(\Omega) \, n \, |\alpha_p|^2, \quad (24)$$

$$S_{a \to p}(n) = \mathrm{d}z \frac{\pi \omega_p \omega}{4\hbar \epsilon_0^2 n^2(\omega_p) n^2(\omega) A_{\mathrm{eff}} L^2} K(|\Omega|, \theta) (m_{\mathrm{th}}(|\Omega|) + 1) \, n \, |\alpha_p|^2. \quad (25)$$

---

[1] Note that $K_\parallel(|\Omega|)$ and $K_\perp(|\Omega|)$ are slightly different in the core and in the cladding of the fiber because of the dopants. Here, we neglect this difference.

Therefore the *net* Raman scattering rates from a coherent pump to Stokes and anti-Stokes modes (containing *n* photons initially) are

$$S(n) = S_{p \to s}(n) - A_{s \to p}(n) = \frac{\pi \omega_p \omega \mathrm{d}z}{4\hbar \epsilon_0^2 n^2(\omega_p) n^2(\omega) A_{\mathrm{eff}} L^2} K(|\Omega|, \theta) \ (n + m_{\mathrm{th}}(|\Omega|) + 1) \ |\alpha_p|^2,$$

(26)

$$A(n) = A_{p \to a}(n) - S_{a \to p}(n) = \frac{\pi \omega_p \omega \mathrm{d}z}{4\hbar \epsilon_0^2 n^2(\omega_p) n^2(\omega) A_{\mathrm{eff}} L^2} K(|\Omega|, \theta) \ (-n + m_{\mathrm{th}}(|\Omega|)) \ |\alpha_p|^2.$$

(27)

When a pump wave is launched in an optical fiber it scatters photons to many Stokes and anti-Stokes modes simultaneously. The variation in the power spectral density $\mathrm{d}\mathcal{S}(z, \omega)$ due to the scattering in the fiber slice $\mathrm{d}z$ is found by multiplying Eqs. (26) or (27) by the photon energy $\hbar \omega$ and summing over the contribution from all the $c/(n(\omega)L)\mathrm{d}\omega$ modes in the interval $[\omega, \omega + \mathrm{d}\omega]$. Therefore the following differential equations hold for Stokes and anti-Stokes radiation, respectively:

$$\frac{\mathrm{d}}{\mathrm{d}z} \mathcal{S}(z, \omega) = \begin{cases} \left[\mathcal{S}(z, \omega) + \frac{\hbar \omega}{2\pi} \left(m_{\mathrm{th}}(|\Omega|) + 1 \right) \right] g(\omega_p, \Omega, \theta) P_p(z) & \text{if } \Omega = \omega_p - \omega > 0 \text{ (Stokes)} \\ \left[\mathcal{S}(z, \omega) - \frac{\hbar \omega}{2\pi} m_{\mathrm{th}}(|\Omega|) \right] g(\omega_p, \Omega, \theta) P_p(z) & \text{if } \Omega = \omega_p - \omega < 0 \text{ (anti-Stokes)} \end{cases}$$

(28)

where

$$\begin{aligned} g(\omega_p, \Omega, \theta) &= \mathrm{sign}(\Omega) \frac{\pi}{4\hbar^2 c^2 \epsilon_0^2} \frac{\omega}{n(\omega_p) n(\omega) A_{\mathrm{eff}}} \left(K_{\parallel}(|\Omega|) \cos^2(\theta) + K_{\perp}(|\Omega|) \sin^2(\theta) \right) \\ &= g_{\parallel}(\omega_p, \Omega) \cos^2(\theta) + g_{\perp}(\omega_p, \Omega) \sin^2(\theta) \end{aligned}$$

(29)

is the *Raman gain*. Eq. (28) is identical to Eq. (1).

Unfortunately, BS and FPS laws cannot be established in the same manner. For FPS, one can start the analysis at the molecular scale, but fourth order perturbation theory is required. In addition, transition amplitudes must be added *coherently* to get the phase matching right (see Sec. 2.3). For BS, a molecular approach is not possible since BS couples light to the excitation of an acoustic wave involving many molecules (see Sec. 2.2).

3.2 Nonlinear quantum field theory

The purpose of the quantum field theory approach is to establish a quantum generalization of the nonlinear Schrödinger equation (NLSE) that governs the propagation of the optical field in a fiber, accounting for dispersion and nonlinear interaction with matter, as well as for spontaneous effects.

3.2.1 Operator equation for nonlinear propagation

Kärtner et al. presented a field theory model of Raman scattering (Kärtner et al., 1994). In this model, a light field $A(z, t)$ is coupled to an harmonic field $Q(z)$, the amplitude of which depends on the position in the fiber. The light field $A(z, t)$ represents the envelope of the E-field oscillating at the carrier frequency ω_0 and is assumed to travel in the fiber at group velocity v_g and with no dispersion. Depending on the dispersion relationship of the field $Q(z)$, it can represent acoustical phonons (if $\omega(q) = v_A q$) or optical photons (if $\omega(q) = \Omega_R$

is independent of q). Coupling to acoustical and optical phonons is responsible for BS and RS, respectively. In (Kärtner et al., 1994) it is assumed that $Q(z)$ is an optical phonon field. Physically $Q(z)$ represents the coordinate of a molecular normal mode of vibration at position z in the fiber. Such a field does not propagate but is nevertheless damped. In order to model the damping (with a rate Γ_R), it is assumed that $Q(z)$ itself is coupled to a large bath of harmonic oscillators at many different frequencies that are at thermal equilibrium. These harmonic oscillators represent other optical and acoustical vibration modes. After eliminating the field $Q(z)$ and the bath variables from the equations, one founds that $A(z,t)$ obeys the nonlinear field equation

$$
\begin{aligned}
\frac{\partial}{\partial z}A(z,t) = & -\frac{1}{v_g}\frac{\partial}{\partial t}A(z,t) + \mathrm{i}(1-f_R)\gamma A^{\dagger}(z,t)A(z,t)A(z,t) \\
& + \mathrm{i}f_R\gamma\int_{-\infty}^{t}h_R(t-t')A^{\dagger}(z,t')A(z,t')\mathrm{d}t'\,A(z,t) + \mathrm{i}\sqrt{f_R\gamma}N_R(z,t)A(z,t),
\end{aligned}
\tag{30}
$$

and the commutation relationship

$$
\left[A(z,t),A^{\dagger}(z,t')\right] = \hbar\omega_0\delta(t-t'),
\tag{31}
$$

where $f_R = 0.18$ (see Sec. 2.3), γ is the nonlinear coefficient (see Sec. 2.3),

$$
h_R(t) = \frac{\Omega_R^2}{\sqrt{\Omega_R^2-(\Gamma_R/2)^2}}\sin\left(\sqrt{\Omega_R^2-(\Gamma_R/2)^2}\,t\right)\exp\left(-(\Gamma_R/2)t\right)\nu(t)
\tag{32}
$$

is the Raman *response function*, and $N_R(z,t)$ is the Raman noise field (see Eqs . (35) and 36 below). In Eq. (32), $\nu(t)$ is the Heaviside step function. The Fourier transform of $h_R(t)$ is called the Raman susceptibility:

$$
\chi_R^{(3)}(\Omega) = \chi_R'(\Omega) + \mathrm{i}\chi_R''(\Omega) = \int_{-\infty}^{\infty}h_R(t)\,\mathrm{e}^{-\mathrm{i}\Omega t}\mathrm{d}t.
\tag{33}
$$

Since $h_R(t) \in \mathbb{R}$ and is normalized such that $\int_{-\infty}^{\infty}h_R(t)\mathrm{d}t = 1$,

$$
\chi_R'(-\Omega) = \chi_R'(\Omega),\quad \chi_R''(-\Omega) = -\chi_R''(\Omega),\quad \chi_R'(0) = 1,\quad \chi_R''(0) = 0.
\tag{34}
$$

The Raman noise operator is such that its Fourier transform

$$
\tilde{N}_R(z,\Omega) = \int_{-\infty}^{\infty}N_R(z,t)\,\mathrm{e}^{-\mathrm{i}\Omega t}\,\mathrm{d}t
\tag{35}
$$

satisfies the following spectral correlations (Boivin et al., 1994; Drummond & Corney, 2001):

$$
\langle\tilde{N}_R^{\dagger}(z,\Omega)\tilde{N}_R(z',\Omega')\rangle = \hbar(\omega_0-\Omega)\frac{|\chi_R''(\Omega)|}{\pi}\left[m_{\mathrm{th}}(|\Omega|)+\nu(\Omega)\right]\delta(z-z')\delta(\Omega-\Omega').
\tag{36}
$$

The second term at the right-hand side of Eq. (30) does not come out of Kärtner's model but has been added phenomenologically to account for the $(1-f_R)$ fraction of the total non linearity that originates in the interaction of light with bound electrons rather than molecular vibrations.

The last term in Eq. (30) is the one responsible for the spontaneous Raman scattering. In order to make the connection with the description given in Secs. 2.1 and 3.1, consider the

propagation of a strong continuous pump field $A_p(z,t) = \sqrt{P_p}$ together with a weak scattered field $A_{\text{sc}}(z,t)$ that is null at the input of the fiber: $A(z,t) = A_p + A_{\text{sc}}(z,t)$. Ignoring all the terms but the last one in Eq. (30) one easily finds that $A_{\text{sc}}(z,t) \approx \mathrm{i}\sqrt{f_R \gamma P_p} \int_0^L N_R(z,t)\mathrm{d}z$. Therefore, the total scattered power is

$$\int_{-\infty}^{\infty} S(L, \omega_0 - \Omega)\mathrm{d}\Omega = \langle A_{\text{sc}}^{\dagger}(z,t) A_{\text{sc}}(z,t)\rangle = f_R \gamma P_p \int_0^L \mathrm{d}z \int_0^L \mathrm{d}z' \langle N_R^{\dagger}(z,t) N_R(z',t')\rangle$$

$$= f_R \gamma P \int_{-\infty}^{\infty} \mathrm{d}\Omega \int_{-\infty}^{\infty} \mathrm{d}\Omega' \int_0^L \mathrm{d}z \int_0^L \mathrm{d}z' \langle \tilde{N}_R^{\dagger}(z,\Omega) \tilde{N}_R(z',\Omega')\rangle$$

Using Eq. (36), one finally gets

$$S(L, \omega = \omega_0 - \Omega) = \hbar(\omega_0 - \Omega) f_R \gamma \frac{|\chi_R''(\Omega)|}{\pi} \left[m_{\text{th}}(|\Omega|) + \nu(\Omega) \right] P_p L. \qquad (37)$$

Comparing this expression with Eq. (5), the Raman gain is found to be related to the imaginary part of the Raman susceptibility by the following relationship:

$$g_{\parallel}(\omega_p, \Omega) = -2 f_R \gamma \chi_R''(\Omega) \qquad (38)$$

According to the Kärtner's model, the Raman gain would be Lorentzian in shape because

$$\chi_R''(\Omega) = \frac{\Omega \Omega_R^2 \Gamma_R}{(\Omega_R^2 - \Omega^2)^2 + \Omega^2 \Gamma^2}, \qquad (39)$$

according to Eqs. (32) and (33). This would be a rough approximation of the actual Raman gain in Fig. 2a. As explained in (Drummond & Corney, 2001), the Raman gain is well fitted by a 10-Lorentzian model. Modifying the quantum field model to couple light to ten Lorentzian vibration modes is trivial: it only changes the shape of the Raman response function $h_R(t)$ in Eq. (32), which becomes a linear superposition of damped sine functions with appropriate oscillation frequencies and damping constants.

With this modification, the quantum propagation equation (30) is able to simulate the spontaneous grow of Stokes and anti-Stokes wave and their amplification. However, Eq. (30) is unable to simulate FPS despite that all the terms (second and third term of the right-hand side) responsible for photon-pair generation are included. This is because phase-matching is of crucial importance for the FPS process and Eq. (30) does not properly deal with the group velocity dispersion of the traveling waves.

3.2.2 Dispersion

Dispersion plays an important role in the physics of spontaneous and stimulated nonlinear effects. The exact dispersion of the fiber can be include in the quantum non linear propagation equation (30) by replacing the first term in the right-hand side

$$-\frac{1}{v_g}\frac{\partial}{\partial t} A(z,t) \qquad (40)$$

by the generalized dispersion operator

$$\mathcal{D}[A(z,t)] = +\mathrm{i} \sum_{a=1}^{\infty} (\mathrm{i})^a \frac{k_a}{a!} \frac{\partial^a}{\partial t^a} A(z,t), \qquad (41)$$

where

$$k_a = \left. \frac{\mathrm{d}^a}{\mathrm{d}\omega^a} k_L(\omega) \right|_{\omega=\omega_0} \tag{42}$$

are the derivatives of the propagation constant $k_L(\omega)$. The dispersion operator can also be written as a convolution integral (Kärtner et al., 1994; Lin et al., 2007)

$$\mathcal{D}[A(z,t)] = \mathrm{i} \int_{-\infty}^{t} h_L(t-t') A(z,t') \mathrm{d}t', \tag{43}$$

where

$$h_L(t) = \frac{1}{2\pi} \int_{-\infty}^{\infty} [k_L(\omega_0 - \Omega) - k_L(\omega_0)] \mathrm{e}^{\mathrm{i}\Omega t} \mathrm{d}\Omega \tag{44}$$

is the *linear* response function of the fiber. Using (43) Eq. (30) reads:

$$\begin{aligned}
\frac{\partial}{\partial z} A(z,t) =& \mathrm{i} \int_{-\infty}^{t} h_L(t-t') A(z,t') \mathrm{d}t' + \mathrm{i}(1-f_R)\gamma A^\dagger(z,t) A(z,t) A(z,t) \\
&+ \mathrm{i}f_R\gamma \int_{-\infty}^{t} h_R(t-t') A^\dagger(z,t') A(z,t') \mathrm{d}t' A(z,t) + \mathrm{i}\sqrt{f_R\gamma} N_R(z,t) A(z,t),
\end{aligned} \tag{45}$$

3.2.3 Brillouin and polarization effects

As mentioned in Sec. 3.2.1, the quantum propagation model couples light to non propagative phonons. Strictly speaking, such a model is unsuitable for describing BS. However, if the propagation length is long enough to consider that momentum conservation (opto-acoustical phase matching) is verified, the phonon field has a well defined oscillation frequency $\Omega_B = 4\pi\, v_A\, \frac{n(\omega_p)}{\lambda_p}$, see Eq. (10). Therefore, the Brillouin Lorentzian gain can be included as an eleventh Lorentzian (ultra-low frequency) contribution to the nonlinear Raman response $h_R(t)$ (Drummond & Corney, 2001).

Eq. (45) only takes into account nonlinear effects that involve photons with the same polarization state. One can generalize the model to take polarization into account (Brainis, 2009; Brainis et al., 2005; Lin et al., 2006; 2007).

3.2.4 Solving the quantum propagation equation

There are two main methods to solve the quantum nonlinear propagation equation.

The first one is using numerical integration and consists in converting Eq. 45 into a set of c-number equations with *stochastic terms* in order to solve them on a computer (Brainis et al., 2005; Kennedy & Wright, 1988). These methods have been first introduced to solve the scalar quantum equation without the Raman effect ($f_R = 0$) to study the squeezing of a quantum soliton (Carter et al., 1987; Drummond & Carter, 1987) and co-polarized FPS (Brainis et al., 2005). It has been then generalized to study different types of *non* co-polarized FPS processes (Amans et al., 2005; Brainis et al., 2005; Kennedy, 1991) and squeezing in birefringent fibers (Kennedy & Wabnitz, 1988), as well as Raman scattering noise (Drummond & Corney, 2001).

The second method consists in linearizing the quantum nonlinear equation around a classical solution such as a continuous pump wave or a soliton in order to derive linear couple mode operator equations that can be solved analytically (Brainis, 2009; Brainis et al., 2007; Lin et al., 2006; 2007). Coupled mode equations are easier to establish from the Fourier transform of Eq. (45). Defining the Fourier components of the wave as

$$\tilde{A}(z,\Omega) = \int_{-\infty}^{\infty} A(z,t) \mathrm{e}^{-\mathrm{i}\Omega t} \mathrm{d}t, \tag{46}$$

one finds that they satisfy the following equation:

$$\frac{\partial}{\partial z}\tilde{A}(z,\Omega) = i[k_L(\omega_0 - \Omega) - k_L(\omega_0)]\tilde{A}(z,\Omega) + i\sqrt{f_R}\gamma\frac{1}{2\pi}\int_{-\infty}^{\infty}\mathrm{d}\omega_1 N_R(z,\Omega - \omega_1)A(z,\omega_1)$$

$$+ i\gamma\frac{1}{(2\pi)^2}\int_{-\infty}^{\infty}\mathrm{d}\omega_1\int_{-\infty}^{\infty}\mathrm{d}\omega_2\chi(\omega_2 - \omega_1)\tilde{A}(z,\omega_1)\tilde{A}(z,\omega_2)\tilde{A}(z,\Omega + \omega_1 - \omega_2),$$

$$(47)$$

where

$$\chi(\Omega) = (1 - f_R) + f_R\,\chi_R(\Omega) \tag{48}$$

is the total third order susceptibility which takes into account both electronic and vibrational non linearity. $\chi(\Omega)$ is a complex function that has the same symmetry properties as $\chi_R(\Omega)$, see Eq. (34)

$$\chi'(-\Omega) = \chi'(\Omega), \quad \chi''(-\Omega) = -\chi''(\Omega), \quad \chi'(0) = 1, \quad \chi''(0) = 0. \tag{49}$$

Using Eq. (31), one finds that the operators $\tilde{A}(z,\Omega)$ satisfy the following commutation relations

$$\left[\tilde{A}(z,\Omega), \tilde{A}^\dagger(z,\Omega')\right] = 2\pi\hbar\omega_0\delta(\Omega - \Omega'). \tag{50}$$

A generalization of Eqs. (47)-(50) that takes into account polarization can be found in (Lin et al., 2007). Linearized coupled mode equations are directly obtained from Eq. (47). Hereafter, the result is given for one and two pump waves. These coupled-mode equations will be used in Sec. 4 to analyze the competition between the RS process and the FPS process.

3.2.4.1 Single pump configuration

Let us assume that that a monochromatic pump wave with frequency $\omega_p = \omega_0$ and spectral amplitude $\tilde{A}(z = 0,\Omega) = 2\pi\sqrt{P_p}\delta(\Omega)$ is launched in the fiber. During the propagation, the pump remains monochromatic but acquires a nonlinear phase modulation: $\tilde{A}(z,\Omega) = 2\pi A_p(z)\delta(\Omega)$. The amount of phase modulation can be derived by injecting this ansatz in Eq. (47). One finds that

$$\frac{\mathrm{d}A_p}{\mathrm{d}z} = i\gamma A_p^\dagger(z)A_p(z)A_p(z). \tag{51}$$

The solution of this equation is

$$A_p(z) = \sqrt{P_p}\mathrm{e}^{i\gamma P_p z}. \tag{52}$$

However, this solution is not a stable solution of Eq. (47). Brillouin, Raman and four-photon scattering, will spontaneously scattered power from the pump to Stokes and anti-Stokes frequencies. Nevertheless, for the calculation of the Stokes and anti-Stokes amplitudes, one can make the assumption that the pump remains *undepleted*, i.e. (52) is approximately valid. Injecting the ansatz

$$\tilde{A}(z,\Omega) = \left[2\pi A_p(z)\delta(\Omega) + \tilde{A}_{\mathrm{sc}}(z,\Omega)\right], \tag{53}$$

and retaining only the terms of highest order in P, one finds that the scattered field $\tilde{A}_{\mathrm{sc}}(z,\Omega)$ satisfies

$$\frac{\partial}{\partial z}\tilde{A}_{\mathrm{sc}}(z,\Omega) = i\ \left[[k_L(\omega_p - \Omega) - k_L(\omega_p)] + B(\Omega)\gamma P_p\right]\tilde{A}_{\mathrm{sc}}(z,\Omega)$$

$$+ i\ \chi(\Omega)\gamma P\mathrm{e}^{i2\gamma P_p z}\ \tilde{A}_{\mathrm{sc}}^\dagger(z,-\Omega) + i\ \sqrt{f_R\gamma P_p}\mathrm{e}^{i\gamma P_p z}\ N_R(z,\Omega),$$

$$(54)$$

where

$$B(\Omega) = \chi(0) + \chi(\Omega) = 1 + \chi(\Omega) = 2 - f_R[1 - \chi_R(\Omega)]. \tag{55}$$

The coefficient $B(\Omega)$ measures the relative strength of the cross-phase modulation of the scattered field by the pump and the self-phase modulation of the pump, see Eq. (52). If Raman scattering is ignored ($f_R = 0$), it takes the usual value $B = 2$. At frequencies close to the pump ($\Omega \to 0$), one also finds $B \approx 2$, because $\chi_R \approx 1 + 0i$. Very far away from the pump frequency ($\Omega \to \infty$), $B \approx 1.82$ because $\chi_r \approx 0 + 0i$ and $f_R = 0.18$. The third term of the Eq. (54) represents a FWM process with a complex coupling coefficient $\chi(\Omega)\gamma P_p$. In Sec. 4, it will be shown that this term is responsible for stimulated FWM, stimulated Raman and Brillouin scattering, as well as spontaneous FPS. One may notice that this term couples each spectral component at $\Omega > 0$ (Stokes) to the symmetric component at frequency $\Omega < 0$ (anti-Stokes), as required by the aforementioned processes. The last term in the right-hand side of Eq. (54) is the source of spontaneous Raman and Brillouin scattering. Since Stokes and anti-Stokes frequencies are always coupled, the coupled-mode equations

$$\frac{\partial}{\partial z} \tilde{A}_{\text{sc}}(z,\Omega) = i \left[[k_L(\omega_p - \Omega) - k_L(\omega_p)] + B(\Omega)\gamma P_p \right] \tilde{A}_{\text{sc}}(z,\Omega)$$

$$+ i \chi(\Omega)\gamma P_p e^{i2\gamma P_p z} \tilde{A}_{\text{sc}}^\dagger(z,-\Omega) + i \sqrt{f_R \gamma P_p} e^{i\gamma P_p z} N_R(z,\Omega), \tag{56}$$

$$\frac{\partial}{\partial z} \tilde{A}_{\text{sc}}(z,-\Omega) = i \left[[k_L(\omega_p + \Omega) - k_L(\omega_p)] + B(-\Omega)\gamma P_p \right] \tilde{A}_{\text{sc}}(z,-\Omega)$$

$$+ i \chi(-\Omega)\gamma P_p e^{i2\gamma P_p z} \tilde{A}_{\text{sc}}^\dagger(z,\Omega) + i \sqrt{f_R \gamma P_p} e^{i\gamma P_p z} N_R(z,-\Omega). \tag{57}$$

must be solved together to solve the propagation problem. These are linear, but inhomogeneous equations. Note that

$$\chi(-\Omega) = \chi^*(\Omega), \qquad \text{and} \qquad B(-\Omega) = B^*(\Omega). \tag{58}$$

3.2.4.2 Dual pump configuration

If two pump waves at frequencies $\omega_{p1} = \omega_0 - \Omega_p$ and $\omega_{p2} = \omega_0 + \Omega_p$ are launched simultaneously in the fiber, the spectral amplitude can be written

$$\tilde{A}(z,\Omega) = 2\pi A_{p1}(z)\delta(\Omega - \Omega_p) + 2\pi A_{p2}(z)\delta(\Omega + \Omega_p) \tag{59}$$

Injecting this ansatz in Eq. 47 shows the the two pumps will interact through nonlinear effects:

$$\frac{dA_{p1}}{dz} = i \left[[k_L(\omega_0 - \Omega_p) - k_L(\omega_0)] + \gamma|A_{p1}|^2 + B(2\Omega_p)\gamma|A_{p2}|^2 \right] A_{p1}(z) \tag{60}$$

$$\frac{dA_{p2}}{dz} = i \left[[k_L(\omega_0 + \Omega_p) - k_L(\omega_0)] + \gamma|A_{p2}|^2 + B(-2\Omega_p)\gamma|A_{p1}|^2 \right] A_{p2}(z) \tag{61}$$

The third terms on the right-hand side are responsible for both cross-phase modulation and stimulated Raman scattering: Eq. (38) shows that

$$iB(\pm 2\Omega_p)\gamma = i \left[2 - f_R[1 - \chi'(\pm 2\Omega_p)] \right] \gamma - f_R \gamma \chi''(\pm 2\Omega_p),$$

$$= i \left[2 - f_R[1 - \chi'(\pm 2\Omega_p)] \right] \gamma + \frac{g_\parallel(\pm 2\Omega_p)}{2}. \tag{62}$$

If the propagation distance L and the initial pump powers P_{p1} and P_{p2} are such that $g_\parallel(2\Omega_p)(P_{p1} + P_{p2})L \ll 1$, power transfer due to stimulated Raman scattering is negligible and the solution of Eqs. (60) and (61) is:

$$A_{p1}(z) = P_{p1} \exp\left[i\left[[k_L(\omega_0 - \Omega_p) - k_L(\omega_0)] + \gamma P_{p1} + \Re[B(2\Omega_p)]\gamma P_{p2}\right] z\right], \qquad (63)$$

$$A_{p2}(z) = P_{p2} \exp\left[i\left[[k_L(\omega_0 + \Omega_p) - k_L(\omega_0)] + \gamma P_{p2} + \Re[B(-2\Omega_p)]\gamma P_{p1}\right] z\right]. \qquad (64)$$

As in the single pump case, such a solution in unstable and light will be spontaneously scattered to other wavelength. To analyze that scattering, we introduce the ansatz

$$\tilde{A}(z,\Omega) = 2\pi A_{p1}(z)\delta(\Omega - \Omega_p) + 2\pi A_{p2}(z)\delta(\Omega + \Omega_p) + \tilde{A}_{sc}(z,\Omega) \qquad (65)$$

in Eq. (47) and only keep the terms of highest order in P_{p1} and P_{p2}. It is found that

$$
\begin{aligned}
\frac{\partial}{\partial z}\tilde{A}_{sc}(z,\Omega) = {}& i\left[[k_L(\omega_0 - \Omega) - k_L(\omega_0)] + B(\Omega - \Omega_p)\gamma P_{p1} + B(\Omega + \Omega_p)\gamma P_{p2}\right]\tilde{A}_{sc}(z,\Omega) \\
& + i\gamma\chi(\Omega - \Omega_p)A_{p1}(z)A_{p1}(z)\tilde{A}_{sc}^\dagger(z, 2\Omega_p - \Omega) \\
& + i\gamma\chi(\Omega + \Omega_p)A_{p2}(z)A_{p2}(z)\tilde{A}_{sc}^\dagger(z, -2\Omega_p - \Omega) \\
& + i\gamma 2\Re\left[\chi(\Omega_p - \Omega)\right]A_{p1}(z)A_{p2}(z)\tilde{A}_{sc}^\dagger(z, -\Omega) \\
& + i\gamma\chi(2\Omega_p)A_{p1}^\dagger(z)A_{p2}(z)\tilde{A}_{sc}(z, -2\Omega_p) + i\gamma\chi(-2\Omega_p)A_{p2}^\dagger(z)A_{p1}(z)\tilde{A}_{sc}(z, 2\Omega_p) \\
& + i\gamma\chi(\Omega_p - \Omega)A_{p1}^\dagger(z)A_{p2}(z)\tilde{A}_{sc}(z, \Omega + 2\Omega_p) \\
& + i\gamma\chi(\Omega - \Omega_p)A_{p2}^\dagger(z)A_{p1}(z)\tilde{A}_{sc}(z, \Omega - 2\Omega_p) \\
& + i\sqrt{f_R\gamma}\left[A_{p_1}(z)N_R(z, \Omega - \Omega_p) + A_{p_2}(z)N_R(z, \Omega + \Omega_p)\right].
\end{aligned}
$$
$$(66)$$

In striking contrast with Eq. (54), the light scattered at frequency $\omega_0 - \Omega$ is not only coupled to the symmetric mode $\omega_0 + \Omega$ but also to six other modes at frequencies: $\omega_0 - 2\Omega_p - \Omega$, $\omega_0 - 2\Omega_p$, $\omega_0 - 2\Omega_p + \Omega$, $\omega_0 + 2\Omega_p - \Omega$, $\omega_0 + 2\Omega_p$, $\omega_0 + 2\Omega_p + \Omega$. As a consequence, there is no way to write down a *closed* set of coupled mode equations for that problem. However, the perturbation theory technique introduced in (Brainis, 2009) can be applied to investigation the quantum regime of scattering (see Sec. 4.2).

4. Coupling between spontaneous scattering processes

When light propagates in an optical fiber, spontaneous RS, BS and FPS take place simultaneously. Several processes may scatter light to the same modes so that it may not be possible the decouple the processes. Hereafter, that point is illustrated in the single and dual pump configuration.

4.1 Single pump configuration

The field evolution in the single pump configuration is fully described by the coupled-mode equations (56) and (57), the solution of which is

$$
\begin{aligned}
\tilde{A}_{sc}(L,\Omega) = {}& \mu_1(L,\Omega)\tilde{A}_{sc}(0,\Omega) + \mu_2(L,\Omega)\tilde{A}_{sc}^\dagger(0,-\Omega) \\
& + i\sqrt{f_R\gamma P}\int_0^L N_R(z,\Omega)\left(\mu_1(L-z,\Omega) - \mu_2(L-z,\Omega)\right)\mathrm{d}z
\end{aligned}
$$
$$(67)$$

$$\tilde{A}_{\text{sc}}(L, -\Omega) = \mu_1(L, -\Omega)\tilde{A}_{\text{sc}}(0, \Omega) + \mu_2(L, -\Omega)\tilde{A}_{\text{sc}}^\dagger(0, \Omega)$$
$$+ \, \mathrm{i}\sqrt{f_R\gamma P}\int_0^L N_R(z, -\Omega)\left(\mu_1(L-z, -\Omega) - \mu_2(L-z, -\Omega)\right)\mathrm{d}z. \quad (68)$$

If $\Omega > 0$, $\tilde{A}_{\text{sc}}(L, \Omega)$ corresponds to the Stokes part of the spectrum and $\tilde{A}_{\text{sc}}(L, -\Omega)$ to the anti-Stokes part. The functions $\mu_1(z, \Omega)$ and $\mu_2(z, \Omega)$ are defined as

$$\mu_1(z, \Omega) = \left[\cosh(g(\Omega)L) + \mathrm{i}\frac{\Delta k(\Omega)}{2g(\Omega)}\sinh(g(\Omega)L)\right]\exp\left(\mathrm{i}\frac{k_L(\Omega) - k_L(-\Omega)}{2}L\right) \quad (69)$$

$$\mu_2(z, \Omega) = \mathrm{i}\frac{\gamma\chi(\Omega)P_p\mathrm{e}^{\mathrm{i}2\gamma P_pL}}{g(\Omega)}\sinh(g(\Omega)L)\exp\left(\mathrm{i}\frac{k_L(\Omega) - k_L(-\Omega)}{2}L\right) \quad (70)$$

where

$$\Delta k(\Omega) = k_L(\omega_p - \Omega) + k_L(\omega_p + \Omega) - 2k_L(\omega_p) + 2\gamma P_p[B(\Omega) - 1] = \Delta k_L(\Omega) + 2\gamma P_p\chi(\Omega) \quad (71)$$

is the total phase mismatch and

$$g(\Omega) = \sqrt{(\chi(\Omega)\gamma P_p)^2 - (\Delta k(\Omega)/2)^2} = \sqrt{-\Delta k_L(\Omega)\gamma P_p\chi(\Omega) - (\Delta k_L(\Omega)/2)^2} \quad (72)$$

is the parametric gain. The square-root in Eq. (72) is chosen such that $\Re(g) > 0$. Comparing with the results of Sec. 2.3, both the phase mismatch parameter and the parametric gain have a modified value due to the *simultaneous* action of FPS and RS. This modification impacts the stimulated FWM (Golovchenko et al., 1990; Vanholsbeeck et al., 2003) as well as spontaneous FPS regime (Brainis et al., 2007; Lin et al., 2006).

The spontaneous regime corresponds to the initial conditions $\langle \tilde{A}_{\text{sc}}^\dagger(0, \Omega)\tilde{A}_{\text{sc}}(0, \Omega)\rangle = 0$, for any value of Ω. The spectral power density $S(L, \omega_p - \Omega)$ at the fiber output can be calculated as follows (Brainis et al., 2005; 2007):

$$S(L, \omega_p - \Omega) = \lim_{\epsilon \to 0}\frac{1}{2\pi\epsilon}\int_{\Omega-\epsilon/2}^{\Omega+\epsilon/2}\int_{\Omega-\epsilon/2}^{\Omega+\epsilon/2}\langle \tilde{A}_{\text{sc}}^\dagger(L, \Omega_1)\tilde{A}_{\text{sc}}(L, \Omega_2)\rangle\mathrm{d}\Omega_1\mathrm{d}\Omega_2. \quad (73)$$

Using Eqs. (67) and (68), one finds (Brainis et al., 2007)

$$\frac{S(L, \omega_p - \Omega)}{\hbar(\omega_p - \Omega)} = \frac{1}{2\pi}\left|\chi(\Omega)\gamma P_pL\right|^2\left|\frac{\sinh(g(\Omega)L)}{g(\Omega)L}\right|^2 + \frac{|\Im[\chi(\Omega)]|\gamma P_p}{\pi}\rho(L, \Omega)\left(m_{\text{th}}(|\Omega|) + \nu(\Omega)\right), \quad (74)$$

where

$$\rho(L, \Omega) = \int_0^L\left|\cosh(g(\Omega)z) + \mathrm{i}\,\text{sign}(\Omega)\frac{\Delta k(\Omega)}{2g(\Omega)}\sinh(g(\Omega)z)\right|^2\mathrm{d}z. \quad (75)$$

The first and second terms in the right-hand side of Eq. (74) represent the photons scattered through the four-photon and Raman processes, respectively. Note that $|\Im[\chi(\Omega)]|\gamma = f_R\gamma|\chi_R''(\Omega)| = |g_\parallel(\omega_p, \Omega)|/2$, see Eq. (38).

In the spontaneous regime ($|g(\Omega)|P_p \to 0$), Eq. (74) reduces to

$$\frac{S(L, \omega_p - \Omega)}{\hbar(\omega_p - \Omega)} = \frac{(|\chi(\Omega)|P_pL)^2}{2\pi}\text{sinc}^2\left(\frac{\Delta k}{2}L\right) + \frac{|g_\parallel(\omega_p, \Omega)|P_pL}{2\pi}\left(m_{\text{th}}(|\Omega|) + \nu(\Omega)\right). \quad (76)$$

The Raman contribution to the scattered light is exactly the one given by Eq. 5: this means that FPS has no impact on RS. The reverse is not true: RS as an influence on FPS since it modifies the total susceptibility $\chi(\Omega)$ appearing in the first term. In absence of RS ($f_R = 0$), $\chi(\Omega) = 1$ and one recovers the spectral density of power given by Eq. (14). Since $-1 < \chi'_R(\Omega) \leq 1$ and $-1.4 < \chi''_R(\Omega) < 1.4$, $|\chi(\Omega)| = \sqrt{(1 - f_R(1 - \chi'_R(\Omega)))^2 + (f_R \chi''_R(\Omega))^2}$ is always close to one. For this reason, spontaneous (not amplified) FPS and RS can be considered has uncoupled phenomena.

If the power is high enough ($|g(\Omega)|P_p L > 1$), amplification of the spontaneous scattering takes place. The general formula (74) is well approximated by

$$\frac{S(L, \omega_p - \Omega)}{\hbar (\omega_p - \Omega)} = \frac{e^{2\Re[g(\Omega)]L}}{8\pi} \left[\left| \frac{\chi(\Omega)\gamma P_p}{g(\Omega)} \right|^2 + \frac{|g_\parallel|(\omega_p, \Omega)|\gamma P_p}{2\Re[g(\Omega)]} \frac{|g(\omega) + \mathrm{i}\, \mathrm{sign}(\Omega)\Delta k/2|^2}{|g(\Omega)|^2} \right]. \tag{77}$$

In striking contrast with the analysis of Sec. 2.1, this result shows that the Raman anti-Stokes wave *grows at the same rate as the Raman Stokes wave* instead of saturating at the power density value $\mathcal{S}(L, \omega_p + |\Omega|) = \frac{\hbar\omega}{2\pi} m_{\text{th}}(|\Omega|)$. This effect is due to the coupling of the RS with the FWM. Its detailed explanation can be found in (Brainis et al., 2007; Coen et al., 2002). On the other hand, the exponential amplification of the Stokes wave is completely quenched at frequencies satisfying $\Delta k_L(\Omega) = 0$ because the gain $g(\Omega)$ vanishes in that case, see Eq. (72) (Golovchenko et al., 1990; Vanholsbeeck et al., 2003).

4.2 Dual pump configuration

In the dual pump configuration, the coupled-mode equations (66) do not form a closed set. For this reason, one cannot write an explicit solution as in Sec. 4.1. To study the spontaneous photon scattering, we apply the first-order perturbation technique introduced in (Brainis, 2009).

We first notice that the first term of the right-hand side of (66) represents the phase evolution of scattered field, including the cross-phase modulation due to the two pumps. This phase modulation has no impact on the population of the frequency modes and can be factored out by writing the total scattered E-field

$$E_{\text{sc}}(z, t) = \sqrt{\frac{\hbar\omega_0}{4\pi\epsilon_0 n_0 c}} \int a(z, \Omega)\, e^{\mathrm{i}[k_L(\omega_0 - \Omega) + B(\Omega - \Omega_p)\gamma P_{p1} + B(\Omega + \Omega_p)\gamma P_{p2}]z} e^{-\mathrm{i}(\omega_0 - \Omega)t} \mathrm{d}\Omega, \tag{78}$$

where $a(z, \Omega)$ is the annihilation operator of the frequency mode $\omega - \Omega$. Because the exact phase evolution of the $a(z, \Omega)$ has been factored out, the z dependence of $a(z, \Omega)$ is only due to the FPS effect (Brainis, 2009). On the other hand, the scattered field can be written as

$$E_{\text{sc}}(z, t) = \frac{1}{2\pi\sqrt{2\epsilon_0 n_0 c}}\, e^{\mathrm{i}k_L(\omega_0)z - \mathrm{i}\omega_0 t} \int \tilde{A}_{\text{sc}}(z, \Omega)e^{\mathrm{i}\Omega t} d\Omega, \tag{79}$$

where we used the fact that $E(z, t) = \sqrt{1/(2\epsilon_0 n_0 c)}A(z, t)e^{\mathrm{i}k_L(\omega_0)z - \mathrm{i}\omega_0 t}$ and Eq. (46). Comparing Eqs. (78) and (79), one sees that

$$\tilde{A}_{\text{sc}}(z, \Omega) = \sqrt{2\pi\hbar\omega_0}\, a(z, \Omega)\, e^{\mathrm{i}[k_L(\omega_0 - \Omega) - k_L(\omega_0) + B(\Omega - \Omega_p)\gamma P_{p1} + B(\Omega + \Omega_p)\gamma P_{p2}]z}. \tag{80}$$

In the following, we make the approximation that $B(\Omega) \approx 2$, see Eq. (55) and $\chi(\Omega) \approx 1$, see Eq. (48). This approximation consists in neglecting the dispersion of the non linearity. Using Eq. (80), one obtains the evolution equation for the annihilation operators:

$$
\begin{aligned}
\frac{\partial}{\partial z} a(z, \Omega) ={}& \mathrm{i}\, \gamma\, P_{p1}\, \mathrm{e}^{-\mathrm{i}\Delta k_{11}(\Omega)z}\, a^\dagger(z, 2\Omega_p - \Omega) + \mathrm{i}\, \gamma\, P_{p2}\, \mathrm{e}^{-\mathrm{i}\Delta k_{22}(\Omega)z}\, a^\dagger(z, -2\Omega_p - \Omega) \\
&+ \mathrm{i}\, 2\gamma\, \sqrt{P_{p1}P_{p2}}\, \mathrm{e}^{-\mathrm{i}\Delta k_{12}(\Omega)z}\, a^\dagger(z, -\Omega) \\
&+ \mathrm{i}\, \gamma\, \sqrt{P_{p1}P_{p2}}\, \mathrm{e}^{\mathrm{i}\Delta k_a z}\, a(z, -2\Omega_p) + \mathrm{i}\, \gamma\, \sqrt{P_{p1}P_{p2}}\, \mathrm{e}^{\mathrm{i}\Delta k_b z}\, a(z, 2\Omega_p) \\
&+ \mathrm{i}\, \gamma\, \sqrt{P_{p1}P_{p2}}\, \mathrm{e}^{\mathrm{i}\Delta k_c z}\, a(z, \Omega + 2\Omega_p) + \mathrm{i}\, \gamma\, \sqrt{P_{p1}P_{p2}}\, \mathrm{e}^{\mathrm{i}\Delta k_d z}\, a(z, \Omega - 2\Omega_p) \\
&+ \mathrm{i}\, \sqrt{\frac{f_R \gamma P_{p1}}{2\pi\hbar\omega_0}}\, \mathrm{e}^{\mathrm{i}[k(\omega_0 - \Omega_p) - k(\omega_0 - \Omega) - \gamma P_{p1}]z} N_R(z, \Omega - \Omega_p) \\
&+ \mathrm{i}\, \sqrt{\frac{f_R \gamma P_{p2}}{2\pi\hbar\omega_0}}\, \mathrm{e}^{\mathrm{i}[k(\omega_0 + \Omega_p) - k(\omega_0 - \Omega) - \gamma P_{p2}]z} N_R(z, \Omega + \Omega_p)
\end{aligned}
\tag{81}
$$

where

$$
\Delta k_{11}(\Omega) = k_L(\omega_0 - \Omega) + k_L(\omega_0 - 2\Omega_p + \Omega) - 2k_L(\omega_0 - \Omega_p) + 2\gamma P_{p1} \tag{82}
$$

$$
\Delta k_{22}(\Omega) = k_L(\omega_0 - \Omega) + k_L(\omega_0 + 2\Omega_p + \Omega) - 2k_L(\omega_0 + \Omega_p) + 2\gamma P_{p2} \tag{83}
$$

$$
\Delta k_{12}(\Omega) = k_L(\omega_0 - \Omega) + k_L(\omega_0 + \Omega) - k_L(\omega_0 - \Omega_p) - k_L(\omega_0 + \Omega_p) + \gamma P_{p1} + \gamma P_{p2} \tag{84}
$$

$$
\Delta k_a(\Omega) = k_L(\omega_0 + 2\Omega_p) + k_L(\omega_0 + \Omega_p) - k_L(\omega_0 - \Omega_p) - k_L(\omega_0 - \Omega) + \gamma P_{p1} - \gamma P_{p2} \tag{85}
$$

$$
\Delta k_b(\Omega) = k_L(\omega_0 - 2\Omega_p) + k_L(\omega_0 - \Omega_p) - k_L(\omega_0 + \Omega_p) - k_L(\omega_0 - \Omega) - \gamma P_{p1} + \gamma P_{p2} \tag{86}
$$

$$
\Delta k_c(\Omega) = k_L(\omega_0 - \Omega - 2\Omega_p) + k_L(\omega_0 - \Omega_p) - k_L(\omega_0 + \Omega_p) - k_L(\omega_0 - \Omega) + \gamma P_{p1} - \gamma P_{p2} \tag{87}
$$

$$
\Delta k_d(\Omega) = k_L(\omega_0 - \Omega + 2\Omega_p) + k_L(\omega_0 - \Omega_p) - k_L(\omega_0 + \Omega_p) - k_L(\omega_0 - \Omega) - \gamma P_{p1} + \gamma P_{p2} \tag{88}
$$

Eq. (81) can be written

$$
\mathrm{i}\hbar \frac{\partial}{\partial z} a(z, \Omega) = [G(z), a(z, \Omega)] + \mathrm{i}\hbar L(z, \Omega), \tag{89}
$$

where

$$
\begin{aligned}
L(z, \Omega) = {}& \mathrm{i}\sqrt{\frac{f_R \gamma}{2\pi\hbar\omega_0}} \Big[\sqrt{P_{p1}}\, \mathrm{e}^{\mathrm{i}[k(\omega_0 - \Omega_p) - k(\omega_0 - \Omega) - \gamma P_{p1}]z} N_R(z, \Omega - \Omega_p) \\
&+ \sqrt{P_{p2}}\, \mathrm{e}^{\mathrm{i}[k(\omega_0 + \Omega_p) - k(\omega_0 - \Omega) - \gamma P_{p2}]z} N_R(z, \Omega + \Omega_p) \Big]
\end{aligned}
\tag{90}
$$

and

$$
\begin{aligned}
G(z) = {} & \frac{\hbar}{2}\gamma P_{p1} \int_{-\infty}^{\infty} d\Omega' e^{-i\Delta k_{11}(\Omega')z}\, a^\dagger(z,\Omega')a^\dagger(z,2\Omega_p - \Omega') + h.c. \\
& + \frac{\hbar}{2}\gamma P_{p2} \int_{-\infty}^{\infty} d\Omega' e^{-i\Delta k_{22}(\Omega')z}\, a^\dagger(z,\Omega')a^\dagger(z,-2\Omega_p - \Omega') + h.c. \\
& + \hbar\gamma\sqrt{P_{p1}P_{p2}} \int_{-\infty}^{\infty} d\Omega' e^{-i\Delta k_{12}(\Omega')z}\, a^\dagger(z,\Omega')a^\dagger(z,-\Omega') + h.c. \\
& + \hbar\gamma\sqrt{P_{p1}P_{p2}} \int_{-\infty}^{\infty} d\Omega' e^{i\Delta k_a(\Omega')z}\, a^\dagger(z,\Omega')a(z,-2\Omega_p) + h.c. \\
& + \hbar\gamma\sqrt{P_{p1}P_{p2}} \int_{-\infty}^{\infty} d\Omega' e^{i\Delta k_b(\Omega')z}\, a^\dagger(z,\Omega')a(z,2\Omega_p) + h.c. \\
& + \hbar\gamma\sqrt{P_{p1}P_{p2}} \int_{-\infty}^{\infty} d\Omega' e^{i\Delta k_c(\Omega')z}\, a^\dagger(z,\Omega')a(z,\Omega' - 2\Omega_p) + h.c. \\
& + \hbar\gamma\sqrt{P_{p1}P_{p2}} \int_{-\infty}^{\infty} d\Omega' e^{i\Delta k_d(\Omega')z}\, a^\dagger(z,\Omega')a(z,\Omega' + 2\Omega_p) + h.c.
\end{aligned}
\tag{91}
$$

In Eq. (89), $L(z,\Omega)$ represents the Raman scattering from both pumps. Raman scattered photons contribute incoherently,

$$
\begin{aligned}
\frac{S_R(L,\omega_p - \Omega)}{\hbar(\omega - \Omega)} = {} & \frac{|g_\parallel(\omega_{p1},\Omega - \Omega_p)|P_{p1}L}{2\pi}\left(m_{\text{th}}(|\Omega - \Omega_p|) + \nu(\Omega - \Omega_p)\right) \\
& + \frac{|g_\parallel(\omega_{p2},\Omega + \Omega_p)|P_{p2}L}{2\pi}\left(m_{\text{th}}(|\Omega + \Omega_p|) + \nu(\Omega + \Omega_p)\right),
\end{aligned}
\tag{92}
$$

to the total scattered photon flux. The $[G(z),a(z,\Omega)]$ part of Eq. (89) represents several FPS processes taking place simultaneously: (i) $2\omega_{p1} \to (\omega_{p1} + \Omega_p - \Omega) + (\omega_{p1} - \Omega_p + \Omega)$, (ii) $2\omega_{p2} \to (\omega_{p2} - \Omega_p - \Omega) + (\omega_{p2} + \Omega_p + \Omega)$, (iii) $\omega_{p1} + \omega_{p2} \to (\omega_0 - \Omega) + (\omega_0 + \Omega)$. To see this explicitly, we writing down the evolution of the quantum state of light in the *interaction* picture. The interaction picture is chosen such that the phase evolution of the modes is part of the operator evolution, while energy transfer from mode to mode is part of the state evolution. In this interaction picture $a^{(I)}(z,\Omega) = a(0,\Omega)$ (Brainis, 2009). Therefore the first order perturbation Dyson expansion gives:

$$
\begin{aligned}
|\psi(L)\rangle = {} & \left(1 + \frac{i}{\hbar}\int_0^L G^{(I)}(z)dz\right)|0\rangle = |0\rangle + \int_{-\infty}^{\infty} d\Omega \\
& \left(\xi_{11}(L,\Omega)|1_\Omega, 1_{2\Omega_p - \Omega}\rangle + \xi_{12}(L,\Omega)|1_\Omega, 1_{-\Omega}\rangle + \xi_{22}(L,\Omega)|1_\Omega, 1_{-2\Omega_p - \Omega}\rangle\right)
\end{aligned}
\tag{93}
$$

where

$$
\xi_{11}(L,\Omega) = i\frac{1}{2}(\gamma P_{p1}L)\, e^{-i\Delta k_{11}(\Omega')\frac{L}{2}}\, \mathrm{sinc}\left(\Delta k_{11}(\Omega')\frac{L}{2}\right)
\tag{94}
$$

$$
\xi_{12}(L,\Omega) = i(\gamma\sqrt{P_{p1}P_{p2}}L)\, e^{-i\Delta k_{12}(\Omega')\frac{L}{2}}\, \mathrm{sinc}\left(\Delta k_{12}(\Omega')\frac{L}{2}\right)
\tag{95}
$$

$$
\xi_{22}(L,\Omega) = i\frac{1}{2}(\gamma P_{p2}L)\, e^{-i\Delta k_{22}(\Omega')\frac{L}{2}}\, \mathrm{sinc}\left(\Delta k_{22}(\Omega')\frac{L}{2}\right).
\tag{96}
$$

The threefold entanglement is a clear signature of the interference between three independent FPS processes. The spectral density of power due to these FPS processes can be deduced from the matrix element $\langle\psi(L)|a^\dagger(0,\Omega)a(0,\Omega)|\psi(L)\rangle$ (Brainis, 2009).

5. Conclusion

In this chapter, the physics of Raman, Brillouin, and four-photon scattering processes in silica fibers has been reviewed, as well as their theoretical modeling. It has been shown that a complete quantum field theory is needed to understand the coupling of theses processes in the stimulated and spontaneous regimes. Two examples of coupling have been discussed. The first one was the coupling of the Raman and four-photon scattering processes in a single pump configuration. In that case, it has been shown that the coupling may have spectacular consequences in the amplified spontaneous regime, where an unexpected exponential growth of the anti-Stokes wave is seen. In the second example, the interaction of three FPS processes in a dual pump configuration has been considered. It has been shown that this configuration leads to the generation of a threefold entangled bi-photon state of light.

Spontaneous scattering processes are of great importance the context of quantum light generation and quantum information processing. The methods presented in the chapter apply to the design of quantum source based on optical fibers: engineering the working principle (usually four-photon scattering processes) and estimating their figure of merit (usually limited by the Raman process).

6. Acknowledgement

7. References

Agrawal, G. P. (2007). *Nonlinear Fiber Optics*, fourth edn, Academic Press, Amsterdam.

Alahbabi, M. N., Cho, Y. T. & Newson, T. P. (2005a). 150-km-range distributed temperature sensor based on coherent detection of spontaneous Brillouin backscatter and in-line raman amplification, *J. Opt. Soc. Am. B* 22(6): 1321–1324.

Alahbabi, M. N., Cho, Y. T. & Newson, T. P. (2005b). Simultaneous temperature and strain measurement with combined spontaneous Raman and Brillouin scattering, *Opt. Lett.* 30(11): 1276–1278.

Amans, D., Brainis, E., Haelterman, M., Emplit, P. & Massar, S. (2005). Vector modulation instability induced by vacuum fluctuations in highly birefringent fibers in the anomalous-dispersion regime, *Opt. Lett.* 30(9): 1051–1053.

Aoki, Y. (1988). Properties of fiber Raman amplifiers and their applicability to digital optical communication systems, *J. Ligthwave Technol.* 6(7): 1225–1239.

Benabid, F., Couny, F., Knight, J. C., Birks, T. A. & Russell, P. S. J. (2005). Compact, stable and efficient all-fibre gas cells using hollow-core photonic crystal fibres, *Nature (London)* 434: 488–491.

Benedek, G. B. & Fritsch, K. (1966). Brillouin scattering in cubic crystals, *Phys. Rev.* 149(2): 647–662.

Bloembergen, N. & Shen, Y. R. (1964). Coupling between vibrations and light waves in Raman laser media, *Phys. Rev. Lett.* 12: 504–507.

Boivin, L., Kärtner, F. X. & Haus, H. A. (1994). Analytical solution to the quantum field theory of self-phase modulation with a finite response time, *Phys. Rev. Lett.* 73(2): 240–243.

Bonfrate, G., Pruneri, V., Kazansky, P. G., Tapster, P. & Rarity, J. G. (1999). Parametric fluorescence in periodically poled silica fibers, *Appl. Phys. Lett.* 75(16): 2356–2358.

Brainis, E. (2009). Four-photon scattering in birefringent fibers, *Phys. Rev. A* 79(2): 023840.

Brainis, E., Amans, D. & Massar, S. (2005). Scalar and vector modulation instabilities induced by vacuum fluctuations in fibers: Numerical study, *Phys. Rev. A* 71(2): 23808.

Brainis, E., Clemmen, S. & Massar, S. (2007). Spontaneous growth of Raman Stokes and anti-Stokes waves in fibers, *Opt. Lett.* 32(19): 2819–2821.

Carter, S. J., Drummond, P. D., Reid, M. D. & Shelby, R. M. (1987). Squeezing of quantum solitons, *Phys. Rev. Lett.* 58(18): 1841.

Coen, S., Wardle, D. A. & Harvey, J. D. (2002). Observation of non-phase-matched parametric amplification in resonant nonlinear optics, *Phys. Rev. Lett.* 89(27): 273901.

Corwin, K. L., Newbury, N. R., Dudley, J. M., Coen, S., Diddams, S. A., Weber, K. & Windeler, R. S. (2003). Fundamental noise limitations to supercontinuum generation in microstructure fiber, *Phys. Rev. Lett.* 90(11): 113904.

Crosignani, B., Di Porto, P. & Solimeno, S. (1980). Influence of guiding structures on spontaneous and stimulated emission: Raman scattering in optical fibers, *Phys. Rev. A* 21(2): 594–598.

Dakin, J., Pratt, D., Bibby, G. & Ross, J. (1985). Distributed optical fibre Raman temperature sensor using a semiconductor light source and detector, *Electron. Lett.* 21(13): 569–570.

Digonnet, M. J. F. (ed.) (2001). *Rare-Earth-Doped Fiber Lasers and Amplifiers*, second edn, Marcel Dekker, New-York.

Dougherty, D. J., Kärtner, F. X., Haus, H. A. & Ippen, E. P. (1995). Measurement of the Raman gain spectrum of optical fibers, *Opt. Lett.* 20(1): 31–33.

Drummond, P. D. & Carter, S. J. (1987). Quantum-field theory of squeezing in solitons, *J. Opt. Soc. Am. B* 4(10): 1565.

Drummond, P. D. & Corney, J. F. (2001). Quantum noise in optical fibers. I. Stochastic equations, *J. Opt. Soc. Am. B* 18(2): 139–152.

Dudley, J. M., Genty, G. & Coen, S. (2006). Supercontinuum generation in photonic crystal fiber, *Rev. Mod. Phys.* 78(4): 1135–1184.

Dyer, S. D., Stevens, M. J., Baek, B. & Nam, S. W. (2008). High-efficiency, ultra low-noise all-fiber photon-pair source, *Opt. Express* 16: 9966.

Fan, J. & Migdall, A. (2007). A broadband high spectral brightness fiber-based two-photon source, *Opt. Express* 15: 2915.

Farahani, M. A. & Gogolla, T. (1999). Spontaneous Raman scattering in optical fibers with modulated probe light for distributed temperature Raman remote sensing, *J. Ligthwave Technol.* 17(8): 1379.

Golovchenko, E., Mamyshev, P. V., Pilipetskii, A. N. & Dianov, E. M. (1990). Mutual influence of the parametric effects and stimulated Raman scattering in optical fibers, *IEEE J. Quantum Electron.* 26: 1815–1820.

Hellwarth, R., Cherlow, J. & Yang, T.-T. (1975). Origin and frequency dependence of nonlinear optical susceptibilities of glasses, *Phys. Rev. B* 11(2): 964–967.

Huy, K. P., Nguyen, A. T., Brainis, E., Haelterman, M., Emplit, P., Corbari, C., Canagasabey, A., Ibsen, M., Kazansky, P. G., Deparis, O., Fotiadi, A., Mégret, P. & Massar, S. (2007). Photon pair source based on parametric fluorescence in periodically poled twin-hole silica fiber, *Opt. Express* 15(8): 4419–4426.

Kärtner, F. X., Dougherty, D. J., Haus, H. A. & Ippen, E. P. (1994). Raman noise and soliton squeezing, *J. Opt. Soc. Am. B* 11(7): 1267–1276.

Kazansky, P. G., Russell, P. S. J. & Takebe, H. (1997). Glass fiber poling and applications, *J. Ligthwave Technol.* 15: 1484–1493.

Kennedy, T. A. B. (1991). Quantum theory of cross-phase-modulational instability: Twin-beam correlations in a $\chi^{(3)}$ process, *Phys. Rev. A* 44: 2113–2123.

Kennedy, T. A. B. & Wabnitz, S. (1988). Quantum propagation: Squeezing via modulational polarization instabilities in a birefringent nonlinear medium, *Phys. Rev. A* 38(1): 563.

Kennedy, T. A. B. & Wright, E. M. (1988). Quantization and phase-space methods for slowly varying optical fields in a dispersive nonlinear medium, *Phys. Rev. A* 38(1): 212–221.

Lee, J. H., Tanemura, T., Kikuchi, K., Nagashima, T., Hasegawa, T., Ohara, S. & Sugimoto, N. (2005). Experimental comparison of a Kerr nonlinearity figure of merit including the stimulated Brillouin scattering threshold for state-of-the-art nonlinear optical fibers, *Opt. Lett.* 30(13): 1698–1700.

Lee, K. F., Chen, J., Liang, C., Li, X., Voss, P. L. & Kumar, P. (2006). Generation of high-purity telecom-band entangled photon pairs in dispersion-shifted fiber, *Opt. Lett.* 31: 1905.

Li, X., Chen, J., Voss, P., Sharping, J. & Kumar, P. (2004). All-fiber photon-pair source for quantum communications: Improved generation of correlated photons, *Opt. Express* 12(16): 3737–3744.

Lin, Q., Yaman, F. & Agrawal, G. P. (2006). Photon-pair generation by four-wave mixing in optical fibers, *Opt. Lett.* 31: 1286.

Lin, Q., Yaman, F. & Agrawal, G. P. (2007). Photon-pair generation in optical fibers through four-wave mixing: Role of Raman scattering and pump polarization, *Phys. Rev. A* 75: 023803.

Mahgerefteh, D., Butler, D. L., Goldhar, J., Rosenberg, B. & Burdge, G. L. (1996). Technique for measurement of the Raman gain coefficient in optical fibers, *Opt. Lett.* 21(24): 2026–2028.

McElhenny, J. E., Pattnaik, R. & Toulouse, J. (2008). Polarization dependence of stimulated Brillouin scattering in small-core photonic crystal fibers, *J. Opt. Soc. Am. B* 25(12): 2107–2115.

Mochizuki, K., Edagawa, N. & Iwamoto, Y. (1986). Amplified spontaneous Raman scattering in fiber Raman amplifiers, *J. Ligthwave Technol.* 4(9): 1328–1333.

Olsson, N. & Hegarty, J. (1986). Noise properties of a Raman amplifier, *J. Ligthwave Technol.* 4(4): 396–399.

Pi, Y., Zhang, W., Wang, Y., Huang, Y. & Peng, J. (2008). Temperature dependence of the spontaneous Brillouin scattering spectrum in microstructure fiber with small core, *Tsinghua Science & Technology* 13(1): 43 – 46.

Rarity, J. G., Fulconis, J., Duligall, J., Wadsworth, W. J. & Russel, P. S. J. (2005). Photonic crystal fiber source of correlated photon pairs, *Opt. Express* 13: 534.

Shelby, R. M., Levenson, M. D. & Bayer, P. W. (1985a). Guided acoustic-wave Brillouin scattering, *Phys. Rev. B* 31(8): 5244–5252.

Shelby, R. M., Levenson, M. D. & Bayer, P. W. (1985b). Resolved forward Brillouin scattering in optical fibers, *Phys. Rev. Lett.* 54(9): 939–942.

Smith, R. G. (1972). Optical power handling capacity of low loss optical fibers as determined by stimulated Raman and Brillouin scattering, *Appl. Opt.* 11(11): 2489–2494.

Stolen, R. H. (1979). Polarization effects in fiber Raman and Brillouin lasers, *IEEE J. Quantum Electron.* 15: 1157–1160.

Stolen, R. H., Lee, C. & Jain, R. K. (1984). Development of the stimulated Raman spectrum in single-mode silica fibers, *J. Opt. Soc. Am. B* 1(4): 652–657.

Stolen, R. & Ippen, E. (1973). Raman gain in glass optical waveguides, *Appl. Phys. Lett.* 22(6): 276–278.

Takesue, H. (2006). Long-distance distribution of time-bin entanglement generated in a cooled fiber, *Opt. Express* 14: 3453.

Vanholsbeeck, F., Emplit, P. & Coen, S. (2003). Complete experimental characterization of the influence of parametric four-wave mixing on stimulated Raman gain, *Opt. Lett.* 28: 1960–1962.

Wait, P. C., Souza, K. D. & Newson, T. P. (1997). A theoretical comparison of spontaneous Raman and Brillouin based fibre optic distributed temperature sensors, *Opt. Commun.* 144(1-3): 17 – 23.

Wardle, D. A. (1999). *Raman Scattering in Optical Fibres*, PhD thesis, University of Auckland.

Yeniay, A., Delavaux, J.-M. & Toulouse, J. (2002). Spontaneous and stimulated Brillouin scattering gain spectra in optical fibers, *J. Lightwave Technol.* 20(8): 1425.
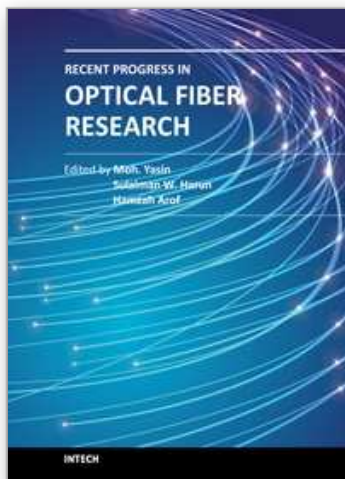
Recent Progress in Optical Fiber Research

Edited by Dr Moh. Yasin

This book presents a comprehensive account of the recent progress in optical fiber research. It consists of four sections with 20 chapters covering the topics of nonlinear and polarisation effects in optical fibers, photonic crystal fibers and new applications for optical fibers. Section 1 reviews nonlinear effects in optical fibers in terms of theoretical analysis, experiments and applications. Section 2 presents polarization mode dispersion, chromatic dispersion and polarization dependent losses in optical fibers, fiber birefringence effects and spun fibers. Section 3 and 4 cover the topics of photonic crystal fibers and a new trend of optical fiber applications. Edited by three scientists with wide knowledge and experience in the field of fiber optics and photonics, the book brings together leading academics and practitioners in a comprehensive and incisive treatment of the subject. This is an essential point of reference for researchers working and teaching in optical fiber technologies, and for industrial users who need to be aware of current developments in optical fiber research areas.

How to reference

In order to correctly reference this scholarly work, feel free to copy and paste the following:

INTECH
open science | open minds